

Native T1 Mapping of the Heart – A Pictorial Review

Philippe Germain^{1,2}, Soraya El Ghannudi¹, Mi-Young Jeung¹, Patrick Ohlmann², Eric Epailly³, Catherine Roy¹ and Afshin Gangi¹

¹Department of Radiology, University Hospital, Strasbourg, France. ²Department of Cardiology, University Hospital, Strasbourg, France.

³Department of Cardiac Surgery, University Hospital, Strasbourg, France.

ABSTRACT: T1 mapping is now a clinically feasible method, providing pixel-wise quantification of the cardiac structure's T1 values. Beyond focal lesions, well depicted by late gadolinium enhancement sequences, it has become possible to discriminate diffuse myocardial alterations, previously not assessable by noninvasive means. The strength of this method includes the high reproducibility and immediate clinical applicability, even without the use of contrast media injection (native or pre-contrast T1). The two most important determinants of native T1 augmentation are (1) edema related to tissue water increase (recent infarction or inflammation) and (2) interstitial space increase related to fibrosis (infarction scar, cardiomyopathy) or to amyloidosis. Conversely, lipid (Anderson–Fabry) or iron overload diseases are responsible for T1 reduction. In this pictorial review, the main features provided by native T1 mapping are discussed and illustrated, with a special focus on the awaited clinical purpose of this unique, promising new method.

KEYWORDS: cardiac magnetic resonance, T1 mapping, edema, myocardial infarction, fibrosis, cardiomyopathy

SUPPLEMENT: Cardiovascular Imaging: Current Developments in Research and Clinical Practice

CITATION: Germain et al. Native T1 Mapping of the Heart – A Pictorial Review. *Clinical Medicine Insights: Cardiology* 2014;8(S4) 1–11 doi: 10.4137/CMC.S19005.

RECEIVED: August 4, 2014. **RESUBMITTED:** October 6, 2014. **ACCEPTED FOR PUBLICATION:** October 7, 2014.

ACADEMIC EDITOR: Thomas Vanhecke, Editor in Chief

TYPE: Review

FUNDING: Authors disclose no funding sources.

COMPETING INTERESTS: Authors disclose no potential conflicts of interest.

COPYRIGHT: © the authors, publisher and licensee Libertas Academica Limited. This is an open-access article distributed under the terms of the Creative Commons CC-BY-NC 3.0 License.

CORRESPONDENCE: germain.philippe7@gmail.com

Paper subject to independent expert blind peer review by minimum of two reviewers. All editorial decisions made by independent academic editor. Upon submission manuscript was subject to anti-plagiarism scanning. Prior to publication all authors have given signed confirmation of agreement to article publication and compliance with all applicable ethical and legal requirements, including the accuracy of author and contributor information, disclosure of competing interests and funding sources, compliance with ethical requirements relating to human and animal study participants, and compliance with any copyright requirements of third parties. This journal is a member of the Committee on Publication Ethics (COPE).

Introduction

The ability to discriminate between T1 and T2 tissue contrast is a unique strength of magnetic resonance imaging. In the past years, new pulse sequences, achievable through breath-hold, were developed, aimed at providing clinically feasible parametric images in which each pixel directly corresponds to the T1 or T2 value of cardiac tissues.¹ Regarding T1 mapping, the MOLLI sequence described in 2004 by Messroghli et al.² and the faster ShMOLLI sequence³ developed by the group of Oxford constitute a real breakthrough, offering robust, fast, and practical quantification of T1 tissue values, immediately available on the scanner console, circumventing the influence of windowing, without a need for manual post-processing. Such a change from visualization to quantification has been described as a true “revolution” of cardiac magnetic

resonance (CMR),⁴ reducing the subjectivity encountered in traditional nonquantitative techniques and providing the ability to differentiate between “normal” and “affected” myocardium. T1 mapping may be performed before (pre-contrast or native T1, reflecting composite water signal from extracellular space and myocytes) but also after contrast media injection (allowing determination of extracellular volume fraction). In this review, we thought to summarize the most salient results obtained with native T1 mapping and to illustrate the potential clinical utility of this technique through a series of cases. Since pre-contrast T1 will only be considered here, the expression “T1” will be used to mean native, pre-contrast T1 in the following paragraphs.

Normal native myocardial T1 values measured with MOLLI at 1.5 T lie between 900 and 1100 ms, but depend on



several technical and physiological parameters. In particular, from 1.5 to 3.0 Tesla field, T1 augmentation was reported to be between 14% and 28% greater. In this article, all presented images were obtained with the basic MOLLI sequence of the Siemens Tx-mapping WIP780, on a 1.5 T Aera scanner. Reported T1 values result from myocardial region of interest (ROI) tracing (being careful to exclude the blood pool as well as the epicardial fat). For the purpose of comparison with published data, mean normal myocardial T1 value determined in our center was 1032 ± 39 ms.

The longitudinal relaxation time T1 is increased in (1) edema resulting from myocardial injury or inflammation, cellular edema, myocyte necrosis and (2) in the case of extracellular space expansion induced by amyloidosis infiltration or by fibrosis, either focal (replacement fibrosis, infarct scar) or diffuse (interstitial fibrosis increased in hypertrophic cardiomyopathy [HCM] and dilated cardiomyopathy [DCM]). Thus, T1 increase is ubiquitous and the use of other complementary imaging sequences such as T2-STIR and late gadolinium enhancement sequences (LGE) is mandatory (summarized in Table 1), as well as interpretation within the clinical context. On the other hand, main causes of T1 reduction include fatty infiltration (lipomatous metaplasia), intracellular sphingolipids overload (Anderson-Fabry), and iron overload diseases. The order of magnitude for the most important T1 alterations recently published is listed in Table 2.

Edema

Area at risk and salvaged myocardium after acute infarction. In 1983, Higgins et al.⁵ demonstrated in dogs that the percentage of water content in an acute myocardial infarction (MI) is approximately 4% greater than that in normal regions and that T1 and T2 values in the area of infarction are greater than those of normal myocardium. This focal T1 increase in water content is related to cellular destruction (infarct core) and to surrounding interstitial edema and may last up to one or two months after acute infarction.⁶ In the case of edema, Ferreira et al demonstrated that T1 mapping was significantly more sensitive than STIR-T2,⁷ and in the setting of experimental acute infarction, Ugander et al showed that both T1 mapping and T2 mapping were similarly sensitive to tissue edema and are closely correlated with the *area*

at risk as assessed by microsphere in animal study.⁸ As it can be seen in Figure 1, in the area of acute MI identified by LGE, the T1 increase is in the range $\approx +20\%$ vs remote myocardium (see Table 2). Edema-related T1 elevation over several standard deviation (SD) above normal values allows for the identification of acute MI with sensitivity and specificity $>90\%$.^{9,10} LGE appears less extensive than increased T1 area but is more specific to myocardial necrosis. The difference between the area at risk (T1 increase) and necrosis (LGE, with a smaller size) corresponds to the salvaged myocardium. In the clinical study of Dal'Armellina et al.¹¹, the diagnostic performance of T1 mapping was similar to that of T2-prep sequence (similar extension of salvaged myocardium). Moreover, T1 mapping seems to be more robust (better reproducibility) than T2-weighted imaging, and increased T1 values have a prognostic significance (weaker segmental function improvement at 6M). The surface area of abnormal myocardium may be visually estimated and manually drawn but this method is prone to subjective over- or underestimation; thus more "objective" criteria, not operator-dependent, should be used, such as pixel count lying over a cut-off value (eg, >3 SD of the mean normal values).⁹ T1 area smaller than LGE area may be observed if imaging is performed too late after the acute event, in the case of poor slice co-localization (misregistration) or in the case of subendocardial infarction.

In the case of *no-reflow* with microvascular obstruction in the infarct core, a pseudo-normalization of T1 values is observed^{10,11} (Fig. 2A), and T1 is even more decreased in the case of hemorrhage (Fig. 2B), owing to methemoglobin accumulation.¹²

Myocarditis and Tako-tsubo syndrome, as well as recent infarction, include an area of edema leading to a focal area of increased T1 and T2 (see Table 2). In acute myocarditis (Fig. 3), this abnormal area is co-localized with regions of LGE¹³⁻¹⁵ because of associated cellular destruction; in contrast, no associated LGE is seen in Tako-tsubo⁷ as illustrated in Figure 4. Interestingly, beyond focal lesions, diffuse increase in myocardial T1 values, although of lower magnitude, is also observed in acute conditions as compared with healthy myocardium^{7,11,13-15} (cf: Table 2). This is particularly salient in cases of acute myocarditis, where the inflammatory process may be diffuse rather than discrete. In this setting,

Table 1. Signal behavior according to different kinds of myocardial diseases.

	DISEASE	T1	T2	LGE
EDEMA	Aborted MI, Tako-Tsubo	Increased	Increased	None
	Acute MI, or myocarditis	Increased	Increased	Present
FIBROSIS	Focal (replacement) or diffuse (interstitial)	Increased	Normal	Detectable if focal

Note: T1 is increased in several categories of cardiac lesions, which may not be discriminated unless T2 and LGE imaging are used as complementary tools (similarly with histology, which relies on various stains to characterize tissue pathology).

Table 2. Range of native T1 values in various pathological conditions.

	DISEASE	FOCAL ALTERATION	DIFFUSE ALTERATION	REFERENCE	NOTA
EDEMA	Acute MI	+18% vs remote +24% vs remote +5 to 9% vs remote ≈+24% vs remote	+3% vs healthy, NS (increased vs healthy) ≈+20% vs healthy	Messroghli et al. ⁹ Ugander ⁸ Dall'Armellina ¹¹ Dall'Armellina ²²	MOLLI 1.5 T, n = 24 MOLLI 1,5 T (9 dogs) ShMOLLI 3 T, n = 41 ShMOLLI 3 T, n = 5
	Acute myocarditis	+12% vs healthy	+7% vs healthy +9% vs controls	Ferreira ^{13,15} Luetkens ¹⁴	ShMOLLI, 1.5 T, n = 60 MOLLI 3 T, n = 24
	Tako-Tsubo	+18% vs healthy	+9% vs healthy	Ferreira ⁷	ShMOLLI 1.5 T, n = 21
FIBROSIS	Chronic MI, scar	+7% vs remote +20% vs remote		Messroghli ⁹ Okur ²⁵	MOLLI 1.5 T, n = 24 MOLLI 3 T, n = 26
	DCM or Heart failure		+16% +4% +2% NS	Puntmann ²⁹ Dass ³⁰ Su ²⁸	MOLLI 3 T, n = 27 ShMOLLI 3 T, n = 19 MOLLI 3 T, n = 102
	HCM		+17% +3%	Puntmann ²⁹ Dass ³⁰	MOLLI 3 T, n = 25 ShMOLLI 3 T, n = 28
	Pressure overload		+7% Mild increase (graph) +3.4%	Bull ²⁶ Sado ³⁹ Lee ²⁷	ShM 1.5 T, 24 AS. ShM 1.5 T, 41HT 21 AS MOLLI 3 T, 80 AS
	Lupus (subclinical) Systemic sclerosis		+9% +5%	Puntmann ³² Ntusi ³³	MOLLI 3 T, n = 33 ShMOLLI, 1.5 T, n = 19
	Amyloidosis		+19% vs healthy +13% ATTR, +17% AL	Karamitsos ³⁵ Fontana ³⁶	ShMOLLI 1.5 T, n = 53 ShMOLLI 1,5 T n = 85,79
	Anderson–Fabry		–9% vs healthy	Sado ³⁸	ShMOLLI 1.5 T, n = 44
OTHER	Iron deposition		–14% vs healthy	Sado ^{39,40}	ShMOLLI 1.5 T, n = 88

Notes: Focal lesions are compared to either remote myocardium (same patient) or healthy myocardium (control series). Diffuse lesions are compared to healthy myocardium (control series). Magnetic field: 1.5 T or 3 T. Sequence: MOLLI or ShMOLLI.

Abbreviations: n, number of patients; MI, myocardial infarction; DCM, dilated cardiomyopathy; HCM, hypertrophic cardiomyopathy; AS, aortic stenosis; HT, hypertension; NS, not significant.

using ShMOLLI at 1.5 T, T1 mapping with a cut-off value of 990 ms offers optimal sensitivity (90%) and specificity (88%) as compared with T2-STIR and LGE imaging. Moreover, the T1 threshold approach is able to diagnose extra cases with small focal islands of myocardial injury, not detected by T2-STIR and LGE imaging.^{13,15}

Myocardial inflammation related to several other diseases, not yet systematically studied up to now, may also provide focal or diffuse increase in T1 values. Systemic disorders that affect the heart, such as sarcoidosis, lupus erythematosus, and systemic sclerosis, are known to induce tissue edema at the acute stage with elevated T2 (and T1) values.¹⁶ In these cases, T1 quantification may be useful to identify cardiac involvement (leading to therapeutic implications) and help assess a prognosis.¹⁷ T1 mapping also seems to have the potential to depict early rejection of transplanted hearts, as shown in Figure 5, which may obviate the need for more invasive endomyocardial biopsy, particularly in the case of primary graft dysfunction.¹⁸

Fibrosis

Fibrosis, which constitutes a common and final pathway in several cardiac diseases, may be discrete, focal (scar), or diffuse (uniform interstitial process).^{19–21} Expansion of the collagen matrix increases the volume of distribution (approximately from 20% to 30%), leading to combined pre-contrast T1 augmentation and greater gadolinium uptake (shorter

post-contrast T1). Thus, focal lesions are assessable by both T1 mapping and LGE techniques. In contrast, in the case of diffuse, uniform T1 alteration, LGE is no longer able to depict abnormal patterns, since no relevant contrast is revealed between one region and another. In this case, T1 mapping circumvents the influence of windowing and reveals its strength, allowing a direct T1 quantification.

Focal replacement fibrosis (scar) in chronic MI. In the chronic stage of MI, edema resolves and is replaced by increased extracellular collagen (fibrous scar). The large area, initially identified with elevated T1 in the acute stage of infarction (edema), is replaced by a smaller area of scar tissue. This phenomenon may explain why both the magnitude and the extent of focal T1 increase are reduced when compared to the acute stage.⁹ However, even 6 months after infarction, some reports showed persistent edema (concomitant T2 increase), which could also account for T1 increase in chronic infarction.²² At 1.5 T, as seen in Figure 6, infarction demonstrated by LGE is seen incompletely on T1 maps and the rate of infarct scar identification was reported to be only 57%,²³ particularly in cases of subendocardial lesion. In contrast, at 3 T, an experimental study in dogs demonstrated that T1 can accurately determine location, size, and transmural of chronic MI, just as well as LGE.²⁴ Similarly, a clinical study conducted in post-infarction patients with low mean ejection fraction (39%, synonymous of large infarction) showed that T1 mapping was able to detect

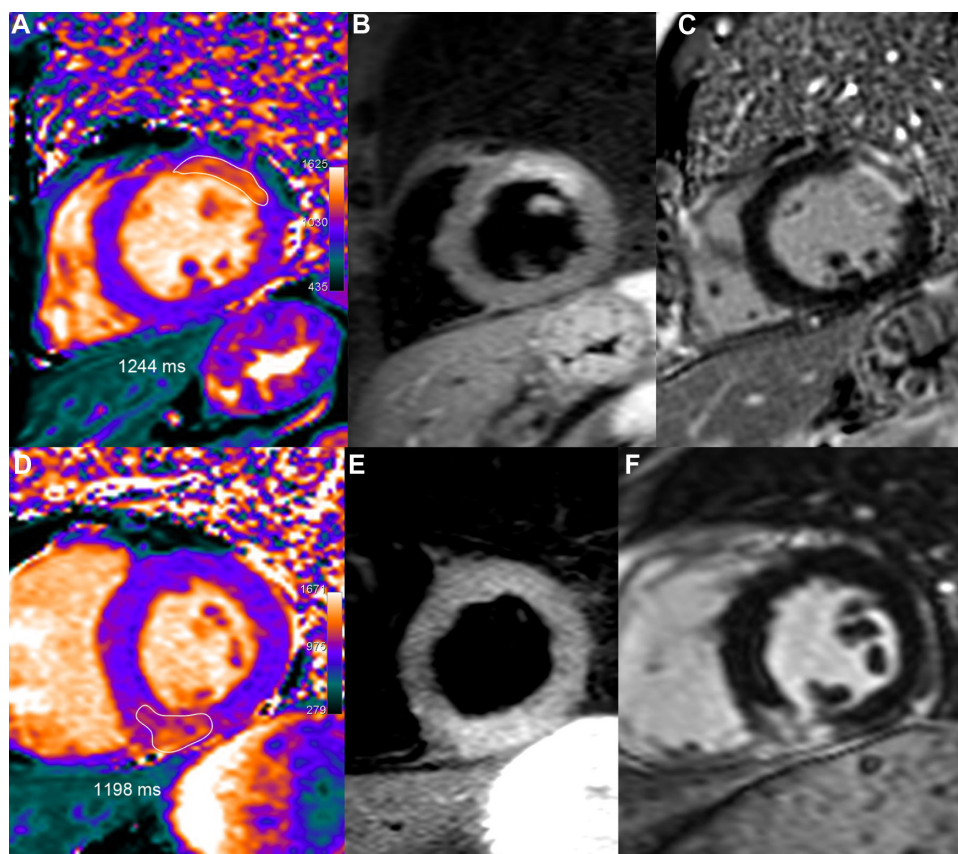


Figure 1. Two examples of acute MI.

Notes: Upper row: 51-year-old male who underwent primary percutaneous coronary intervention (PCI) for an occluded obtuse marginal. After one week, T1 mapping (A) showed increased T1 values (1244 ms, ie, +21% or +5.5 SD vs remote myocardium) in the area of the anterior wall corresponding to the edema depicted by T2-STIR (B), with a larger extent than on LGE imaging (C). Lower row: 52-year-old male presenting an acute inferior infarction related to a right coronary occlusion treated by PCI. Peak troponin I reached 13. At the third day, T1 mapping (D) demonstrated an inferior transmural T1 increase (1198 ms, ie, +15%, or +4.1 SD vs remote myocardium) in the same area than T2-STIR (E) and slightly greater than on LGE imaging (F).

chronic scar tissue caused by chronic MI with 95% sensitivity and 97% specificity, suggesting that accurate diagnosis could be reliably assessed even without LGE imaging,²⁵ but this preliminary report needs to be confirmed.

Another added benefit of T1 mapping in old infarcts, illustrated in Figure 7, is a better view of *lipomatous metaplasia*, with noticeable T1 decrease in the fatty replacement area located within the infarct core.^{10,22}

Diffuse interstitial fibrosis, cardiomyopathy. Myocardial fibrosis is composed of increased deposits of extracellular collagen associated with extracellular matrix expansion. Unlike replacement fibrosis, interstitial fibrosis may be reversible and is a target for treatment (eg, aldosterone).¹⁷ Histological markers of fibrosis have been shown to correlate with increased myocardial stiffness and impaired diastolic function, which are in turn associated with clinical vulnerability and adverse outcome.¹⁷ In recent years, a major interest in T1 mapping has focused on the significant correlation between the degree of fibrosis and increased T1 relaxation time.^{17,19–21} Reported correlations between histological collagen volume fraction determined from biopsy samples obtained during surgery for aortic valve replacement and T1 were good, with $r = 0.65$ ²⁶ and $r = 0.78$.²⁷

In patients with cardiomyopathies, heart failure, or aortic stenosis, four studies found significant myocardial T1 increase (presumably related to interstitial fibrosis) when compared to controls (cf: Table 2), but one other work (performed in heart failure patients) found a not significant +2% T1 increase.²⁸ Puntmann et al reported the strongest difference with $\approx +16\%$ T1 increase in the septum. This T1 increase was correlated to left ventricular (LV) remodeling and systolic dysfunction in DCM patients and was correlated to LV mass index in HCM patients.²⁹ Comparison of area under the curve (Receiver operating characteristic (ROC) analysis) showed that native T1 provided the best distinction between controls and patients with cardiomyopathy (as compared with post-contrast T1). Bull et al reported a +7% T1 augmentation in patients with aortic stenosis.²⁶ T1 increase was less pronounced in the studies of Dass et al.³⁰ ($\approx +3\%$, with changes being borderline if using ROI excluding LGE-positive regions) and of Lee et al.²⁷ (+3.4% in patients with aortic stenosis). In fact, fibrosis involvement, visually perceivable as specific hyper-enhanced foci in HCM (Fig. 8) or quantified as a diffuse process on T1 quantification in DCM (Fig. 9), seems to appear inconsistently on T1 maps. The imperfect concordance between native T1 mapping and LGE imaging

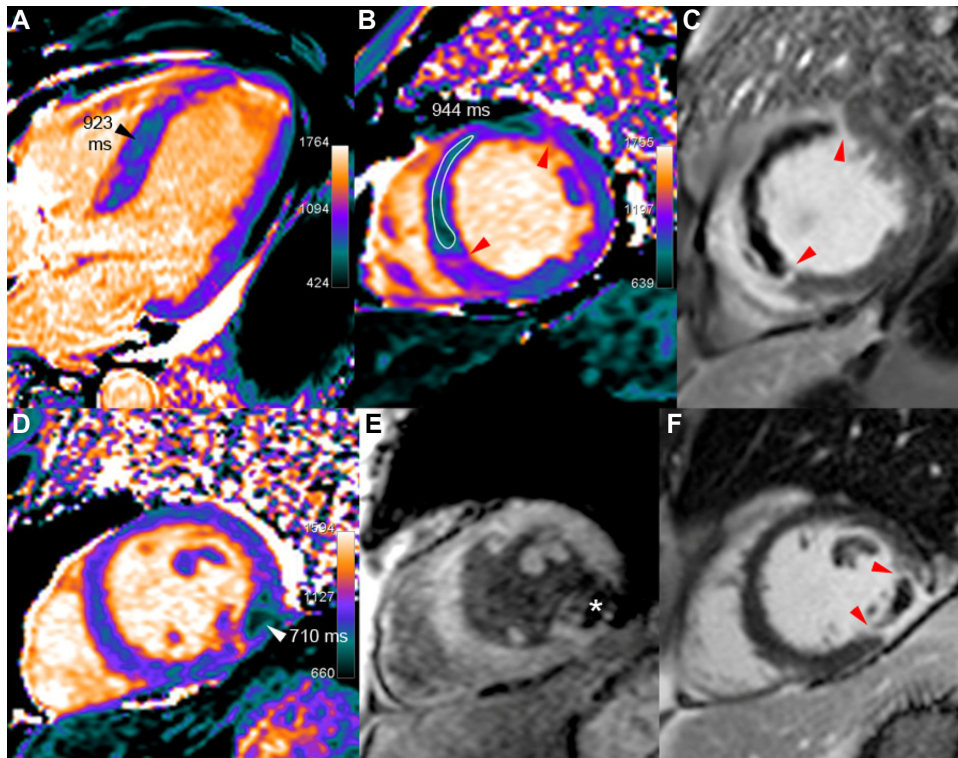


Figure 2. Acute MI with no-reflow and with hemorrhage. **Notes:** (a) Upper row: 60-year-old male at the fifth day of an extensive acute septal STEMI, treated by left anterior descending artery (LAD) stenting for proximal occlusion. T1 maps (A and B) show low T1 values (in the range of 930 ms vs 1060 ms in the remote lateral myocardium) in the large *no-reflow* area extending to almost the entire septum, leaving a thin rim of hyper-enhancement on LGE images (C), confined to the periphery of the infarcted area (red arrow-heads). (b) Lower row: 54-year-old male, six days after acute lateral infarction because of the occlusion of the obtuse marginal branch, revascularized with a stent. Two concordant arguments are in favor of hemorrhage within the infarct core surrounded by post-contrast hyper-enhancement (red arrow-head in F): markedly reduced T1 (710 ms) and strongly reduced signal on T2*-weighted GRE imaging (TE 24 ms), with T2* calculated at 12 ms (white star in E).

for detecting *focal* replacement fibrosis may be explained by the distinct significance of both imaging methods, since LGE (as well as post-contrast T1 mapping) reflects only extracellular space whereas native T1 mapping reflects a composite of both intra- and extracellular compartments.³⁰ Imperfect identification of *diffuse* fibrosis in cardiomyopathies, with large inter-individual

overlap between patient groups, probably results from the limited magnitude of T1 alterations in some fibrotic tissue at 1.5 T or even at 3 T, which may be better discriminated with improved sequences or at higher field strength.³⁰

Several other diseases involving diffuse myocardial fibrosis and impaired diastolic function may reveal increased

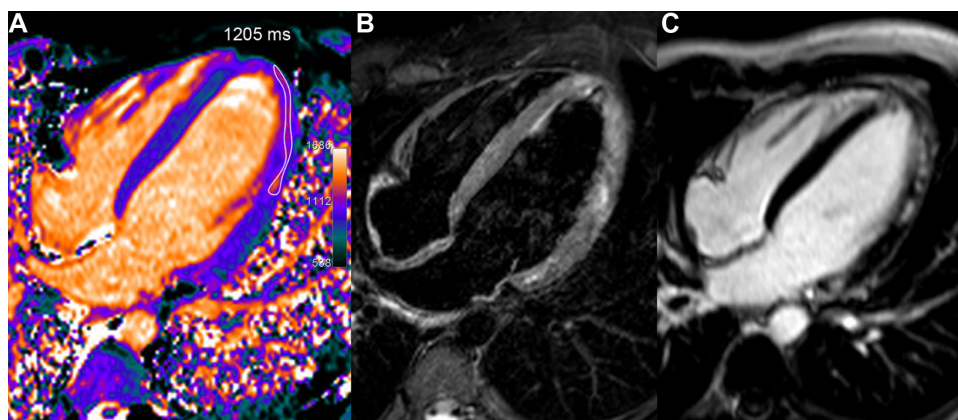


Figure 3. Acute myocarditis in a young 22-year-old male with troponin I rise up to 34 and recent history of gastro-enteritis. T1 map (A), obtained one week after the acute chest pain, shows a rim of high T1 values in the mid and distal lateral walls (1205 ms, ie, +15% or +4.1 SD vs 1044 ms in the septum). T2-STIR imaging (B) found a similar high signal area in several parts of the lateral wall and at the apex. Corresponding LGE image (C) depicts more clearly the cluster of sub-epicardial hyper-enhanced foci in the same location.

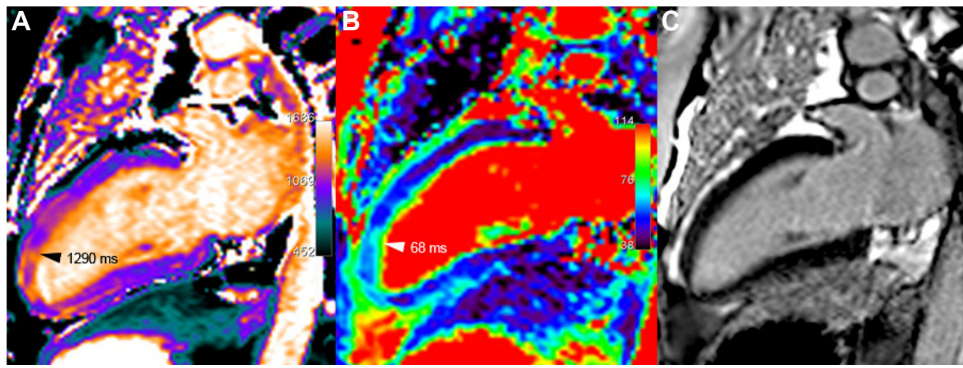


Figure 4. Tako-tsubo syndrome, in a 74-year-old female who presented an anaphylactic shock during orthopedic surgery, requiring the administration of adrenalin, followed by heart failure (EF 40% with anterior-apical dyskinesia). At the time of imaging, 11 days after the acute event, systolic dysfunction has almost disappeared with mild persistent segmental hypokinesia, but anterior distal myocardial edema remains still visible on both T1 (A) and T2 (B) mapping, whereas no abnormal signal enhancement is seen in the corresponding area, using LGE (C).

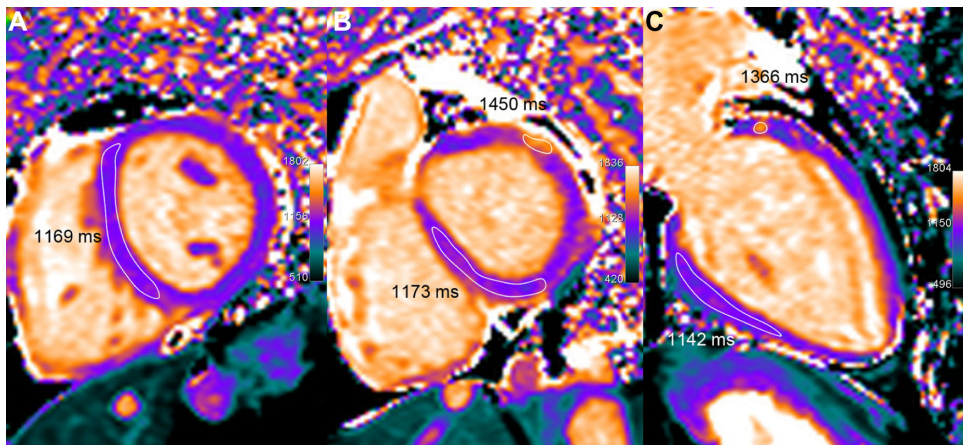


Figure 5. A 67-year-old patient with heart transplantation 5 years ago, presenting clinical and histologic signs of acute rejection. LV volumetric (70 mL/m²) and ejection fraction (60%) are preserved and LGE does not show significant abnormality but T1 mapping demonstrates definitely elevated T1 values (in the range of 1160 ms, ie, +12% or +3.2 SD as compared with normal T1 values in healthy subjects). Moreover, a small nodular of even higher T1 increase (approx. 1400 ms) is seen in the anterior-basal wall. Concomitant T2 elevation (62 ms) suggests an inflammatory process rather than a diffuse interstitial fibrosis.

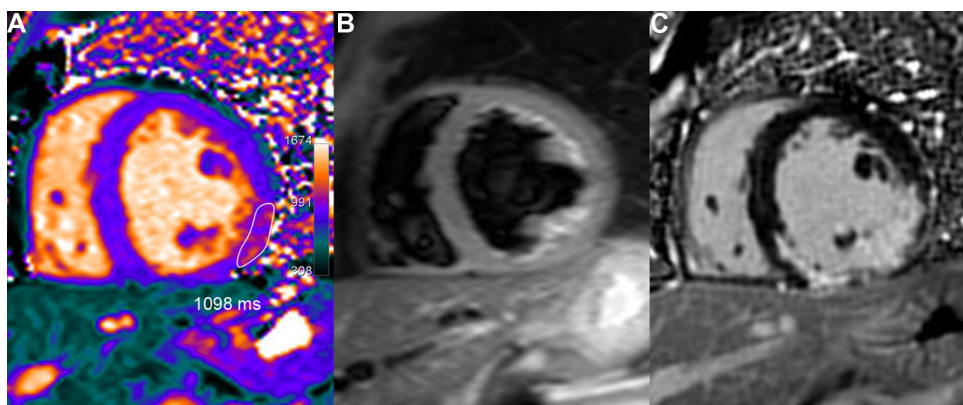


Figure 6. Chronic inferior-lateral MI partially depicted by native T1 mapping. Fibrous infarct scar appears as a limited residual area of mildly elevated T1 values in the T1 map (A) (1098 ms ie, +9% or +2.3 SD vs remote septal wall), covering only partially the much larger area of LGE (C). Lateral wall dyskinesia and low ejection fraction (41%) may explain some signal enhancement around the inferior papillary muscle because of blood stagnation in the T2-STIR image (B).

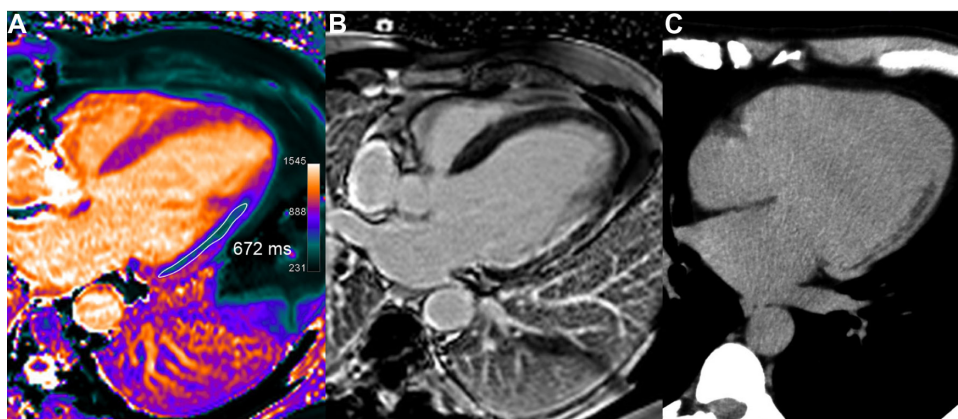


Figure 7. Chronic lateral infarction with lipomatous metaplasia. In this 50-year-old patient with previous lateral infarction 5 years ago, T1 mapping (A) shows an extensive subendocardial area of low T1 values (in the range of 672 ms, ie, -34% or -8.7 SD vs remote septal wall) resulting from fatty replacement, not identified on LGE image (B) but corroborated by fat suppression techniques and by CT scan (C).

myocardial T1: diabetic cardiomyopathy, systemic or pulmonary hypertension, chronic renal disease, valvular heart disease, arrhythmogenic right ventricular cardiomyopathy, atrial fibrillation, and adult congenital heart disease.³¹ In patients with stable systemic lupus erythematosus, T1 increase ($+9\%$), attributed to fibrosis rather than edema, was the best parameter to separate normal subjects from lupus patients.³² In patients with long standing systemic sclerosis (SSc) but without clinical sign of cardiac involvement, a $+5\%$ T1 increase was found as compared with controls. The volume fraction of T1 >990 ms (cut-off for detection of edema with ShMOLLI at 1.5 T) was 52% (vs 3% in controls). These T1 abnormalities were considered to represent a combination of low-grade chronic inflammation and diffuse myocardial fibrosis.³³

Infiltrative, overload, and other cardiac diseases. Even before the advent of T1 mapping, systemic light-chain (AL) amyloidosis was recognized as a typical etiology of markedly elevated myocardial T1 values.³⁴ In a series of 53 patients with biopsy-proven AL amyloidosis, Karamitsos et al demonstrated that T1 values correlated well with markers of systolic and diastolic dysfunction and were 19% higher than those in healthy

subjects, with minimal overlap between groups.³⁵ This was concordant with the presence of typical LGE pattern or with abnormal myocardial to blood pool signal suppression pattern indicative of diffuse myocardial infiltration (Fig. 10). In patients with transthyretin cardiac amyloidosis, T1 elevation was not found to be as high as in AL amyloidosis ($+13\%$ and $+17\%$, respectively), but the area under the ROC curve was similar in both conditions (0.85 and 0.84, respectively).³⁶ The great advantage of T1 mapping here is to be assessable even in patients with severe renal impairment precluding gadolinium chelates injection. Other foreseen advantages of T1 quantitation, as continuous metrics rather than a “binary” visual diagnosis provided by LGE, lie in the possible estimation of a patient’s prognosis and possible interesting tools for treatment monitoring.³⁷

In contrast to previous causes of T1 increase, the London Heart Hospital group reported marked T1 lowering in two kinds of pathologies, both accessible in specific therapy: Anderson–Fabry (Fig. 11) and iron overload diseases. Fabry disease is a rare but underdiagnosed lipid disorder with accumulation of intracellular glycosphingolipids. Mean septal T1 was

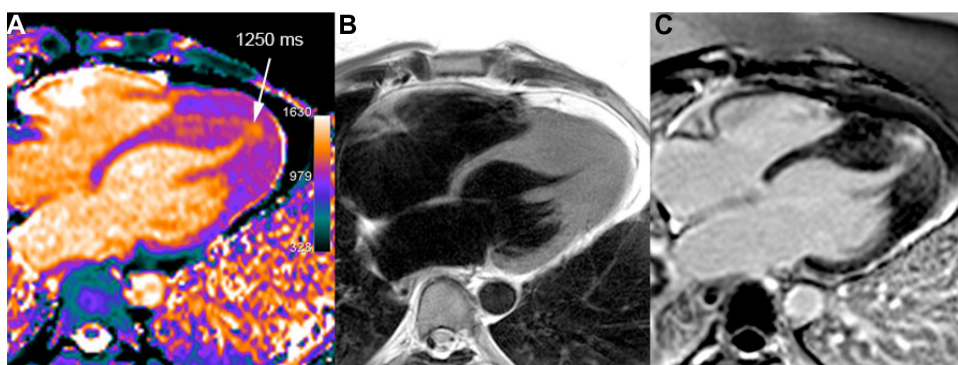


Figure 8. Apical HCM in a 40-year-old man. T1 mapping (A) shows an area of elevated T1 values in the apical and septal distal thickened walls (white arrow) reaching up to 27 mm (diastolic TSE-Blade image – B). A large area of mid-wall patchy heterogeneous fibrosis is seen in the same area on LGE image (C).

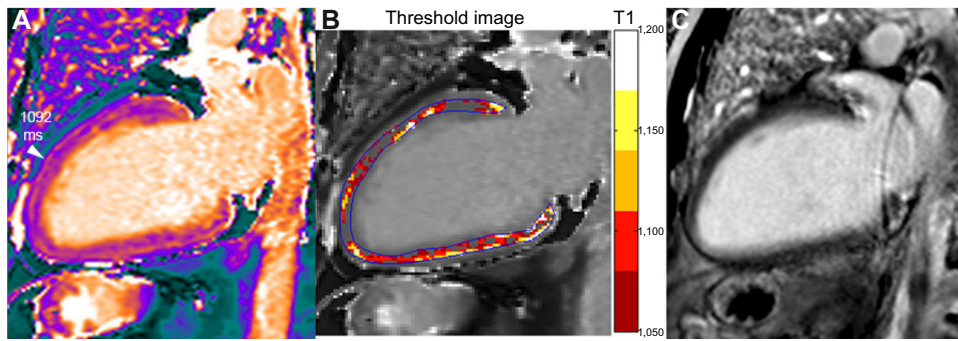


Figure 9. A 62-year-old male with DCM and left bundle branch block (LVEDVI 135 mL/m², EF 25% and normal coronary angiography). Small scattered slightly increased T1 areas are seen in the T1 map (A), but no corresponding abnormal area is seen in the LGE image (C). Signal measurement demonstrates overall T1 increase (1122 ms ie, +9% or +2.3 SD vs healthy myocardium). In contrast to the case of diffuse myocardial edema shown in Figure 5, T1 increase is not associated here with elevated T2 (in the range 51 ms), thus T1 augmentation is consistent with diffuse interstitial fibrosis. Mapping of pixels exceeding a threshold value (T1 >1050 ms in the example shown in B) demonstrates the extent and location of abnormal myocardial area (non-ischemic pattern distribution in this case with DCM).

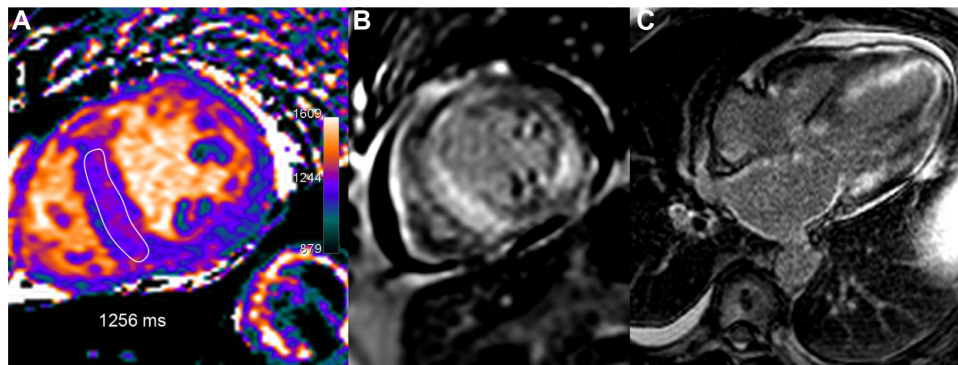


Figure 10. A 66-year-old male with AL amyloidosis, heart failure, and marked restrictive echocardiographic pattern. T1 map (A) shows a heterogeneous T1 increase with septal values in the range of 1256 ms, ie, +22% or +5.7 SD vs healthy myocardium. Typical diffuse subendocardial hyper enhancement is seen on LGE images (B, C).

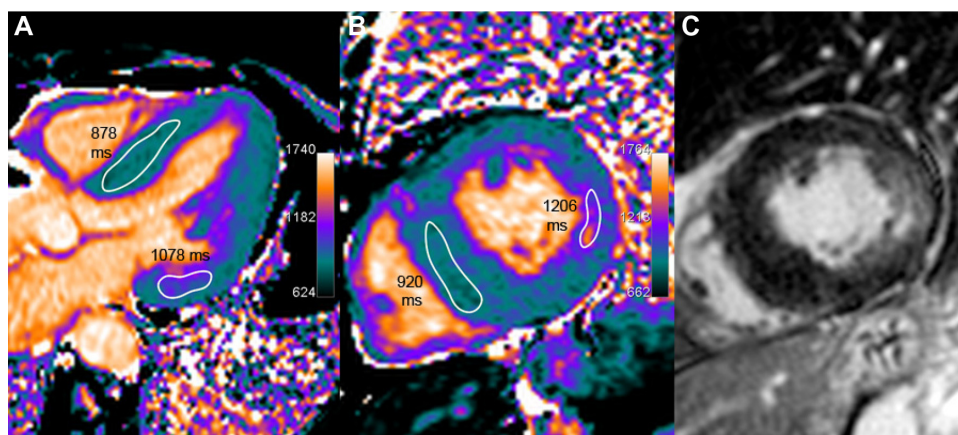


Figure 11. A 64-year-old female with Anderson–Fabry disease. The septum thickness is increased, up to 17 mm (left ventricular mass index 95 g/m²). Myocardial T1 is uniformly low (in the range of 900 ms, as seen on five-chamber and short axis slices in A and B), which is consistent with sphingolipids deposition in this patient. A typical feature of patchy fibrotic involvement of the lateral basal wall is seen with focal T1 pseudo-normalization or even slight increase (approximately 1150 ms) and co-localized signal increase on LGE imaging (C).

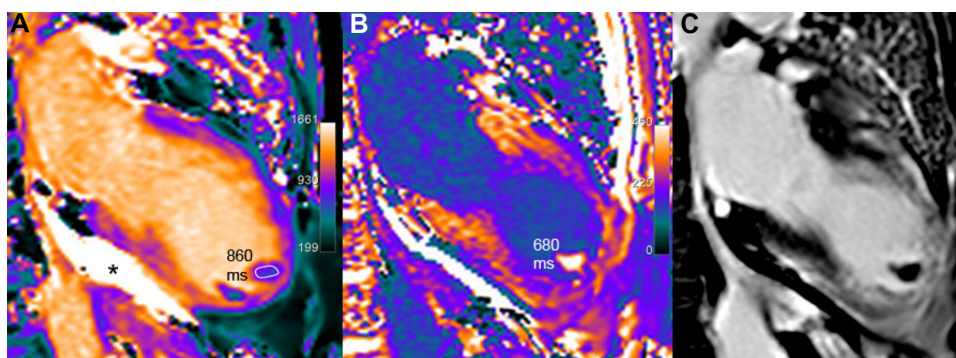


Figure 12. Two apical thrombi (maximal long axis 16 mm) are seen at the apex of the left ventricle in this 69-year-old patient with large apical dyskinesia following LAD occlusion. Native T1 values in the thrombus are lower than myocardial T1 values (A). On post-contrast scan (B), T1 values are mildly reduced (680 ms vs 860 ms), probably because of partial volume effect with the blood pool. Corresponding LGE image (C) confirms infarction and thrombi. T1 value is 2100 ms in the pericardial effusion (black star in A) with no change after gadolinium injection.

reduced by 9% in these patients, and interestingly T1 reduction allowed for an efficient discrimination between Fabry disease and several other causes of left ventricular hypertrophy, with no overlap. T1 correlated inversely with wall thickness and was abnormal in 40% of subjects even without left ventricular hypertrophy (LVH).³⁸ In the case of post-gadolinium contrast enhancement in the postero-lateral wall (a typical feature of this disease), T1 pseudo-normalization or augmentation was focally observed (effect of replacement fibrosis exceeding the fatty-related T1 decrease).

According to the same authors, cardiac iron overload (in transfusion-dependent patients, mostly including thalassemia major) seems to induce even greater T1 reduction. In these patients, T1 was reduced by -14% and T1 strongly correlated with T2* ($r = 0.79$). No patient with low T2* had normal T1, but 32% of patients with normal T2* (>20 ms) presented T1 lowering beyond 2 SD.^{39,40} Similar results and similar correlation between T1 and T2* ($r = 0.83$) were reported by Feng et al.⁴¹, indicating that T1 can be used reliably to assess myocardial iron and that T1 may help plan and monitor iron-chelating treatments.

Finally, aside from previously enumerated myocardial alterations, it is interesting to know that the order of magnitude of T1 values in adipose tissue (paracardiac fatty fringes, lipoma) and in pericardial effusion (Fig. 12) is, respectively, less than 500 and greater than 2000 ms (depending on chemical composition and shorter for protein-rich transudate or abscesses as compared with transudate). Apart from ischemia and cardiomyopathies, T1 mapping reports are scarce for other pathological conditions such as cardiac masses, thrombi (Fig. 12), or tumors (Figs. 13 and 14), but case reports have been published for myxoma,⁴² calcified mitral pseudocyst,⁴³ and lipomatous hypertrophy of the atrial septum.⁴⁴

Conclusion

At present time, pre-contrast T1 mapping has not yet become the “non invasive biopsy” mentioned by Kramer.⁴⁵ However, T1 mapping is already a useful tool for daily diagnostic in several conditions such as amyloidosis, Fabry, and iron overload diseases. Moreover, several reports suggest that in the future, it might become possible to rely on native T1 mapping

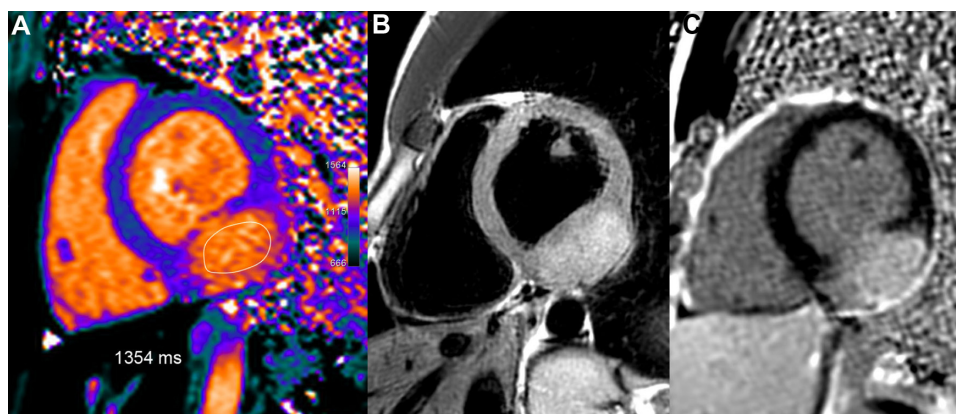


Figure 13. Large inferior-lateral mass (25 mm thick) in a 21-year-old female with atypical symptoms. T1 mapping shows strongly increased T1 values in this tumor, similar to the blood pool T1 values, in the range of 1354 ms, ie, +31% or +8.3 SD vs remote normal septum. Concomitant high T2 signal pattern (B) and marked LGE in this structure (C) suggest a hyper-vascularized tumor.

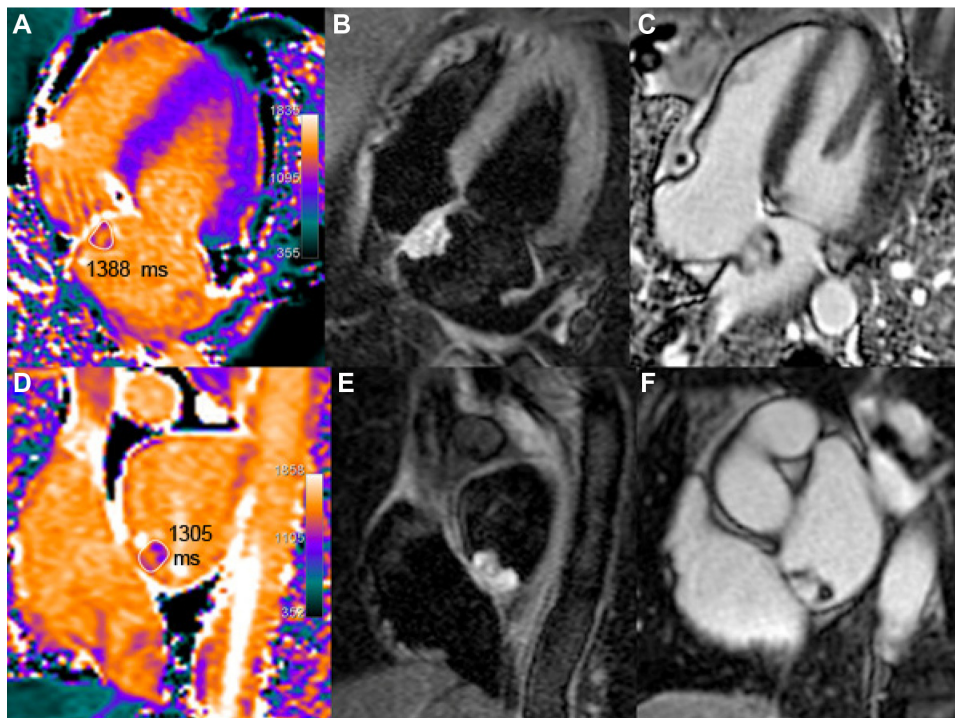


Figure 14. Left atrial myxoma in a 60-year-old female. In the T1 maps (A, D), the T1 value of the tumor is increased (≈ 1350 ms, ie, +25% or +6.9 SD as compared with the septum). High signal of the mass is seen on the corresponding STIR-T2 images (B, E) and in the post-contrast LGE images (heterogeneous pattern in C and F).

instead of LGE imaging for accurate diagnosis of myocarditis and acute or chronic MI, particularly in patients with severe renal impairment precluding gadolinium contrast injection. Tissue characterization in subclinical cardiac injury involving diffuse fibrosis is another awaited clinical application, but overlap remains quite large with normal T1 values. T1 mapping is evolving rapidly and still requires methodological standardization. Objective quantification of abnormal myocardium with threshold-based T1 analysis (areas of injury) will probably help this highly reproducible and minimally operator-dependent technique to better define the prognosis and contribute to monitoring therapy in various myocardial diseases.

Acknowledgments

Authors thank the team of developers of the Siemens Quantitative Cardiac Parameter Mapping (WIP780): B Spottiswoode, A Greiser, C Glielmi, S Giri and R Kroeker and Mrs Ninon Teissier for English editing.

Author Contributions

Conceived and designed the experiment: PG, SE. Analyzed the data: PG, SE. Wrote the first draft: PG. Contributed to the writing: SE, MJ. Agree with results and conclusions: PO, EE, CR, AG. Developed structure and arguments: PG, SE, MJ. Made critical revisions: PG, SE, MJ. All authors reviewed and approved of the final manuscript.

REFERENCES

- Salerno M, Kramer CM. Advances in parametric mapping with CMR imaging. *JACC Cardiovasc Imaging*. 2013;6(7):806–22.
- Messroghli DR, Radjenovic A, Kozerke S, Higgins DM, Sivananthan MU, Ridgway JP. Modified Look-Locker inversion recovery (MOLLI) for high-resolution T1 mapping of the heart. *Magn Reson Med*. 2004;52(1):141–6.
- Piechnik SK, Ferreira VM, Dall'Armellina E, et al. Shortened Modified Look-Locker Inversion recovery (ShMOLLI) for clinical myocardial T1-mapping at 1.5 and 3 T within a 9 heartbeat breathhold. *J Cardiovasc Magn Reson*. 2010;19(12):69.
- Nagel E, Narula J. Evolution and revolution in CMR imaging. *JACC Cardiovasc Imaging*. 2013;6(7):837–8.
- Higgins CB, Herfkens R, Lipton MJ, et al. Nuclear magnetic resonance imaging of acute myocardial infarction in dogs: alterations in magnetic relaxation times. *Am J Cardiol*. 1983;52(1):184–8.
- Goldfarb JW, Arnold S, Han J. Recent myocardial infarction: assessment with unenhanced T1-weighted MR imaging. *Radiology*. 2007;245(1):245–50.
- Ferreira VM, Piechnik SK, Dall'Armellina E, et al. Non-contrast T1-mapping detects acute myocardial edema with high diagnostic accuracy: a comparison to T2-weighted cardiovascular magnetic resonance. *J Cardiovasc Magn Reson*. 2012;14:42.
- Ugander M, Bagi PS, Oki AJ, et al. Myocardial edema as detected by pre-contrast T1 and T2 CMR delineates area at risk associated with acute myocardial infarction. *JACC Cardiovasc Imaging*. 2012;5(6):596–603.
- Messroghli DR, Walters K, Plein S, et al. Myocardial T1 mapping: application to patients with acute and chronic myocardial infarction. *Magn Reson Med*. 2007;58(1):34–40.
- Darach o h-Ici DO, Jeuthe S, Al-Wakeel N, et al. T1 mapping in ischaemic heart disease. *Eur Heart J Cardiovasc Imaging*. 2014;15(6):597–602.
- Dall'Armellina E, Piechnik SK, Ferreira VM, et al. Cardiovascular magnetic resonance by non contrast T1-mapping allows assessment of severity of injury in acute myocardial infarction. *J Cardiovasc Magn Reson*. 2012;6(14):15.
- Pedersen SF, Thrysoe SA, Robich MP, et al. Assessment of intramyocardial hemorrhage by T1-weighted cardiovascular magnetic resonance in reperfusion acute myocardial infarction. *J Cardiovasc Magn Reson*. 2012;14:59.
- Ferreira VM, Piechnik SK, Dall'Armellina E, et al. T1 mapping for the diagnosis of acute myocarditis using CMR: comparison to T2-weighted and late gadolinium enhanced imaging. *JACC Cardiovasc Imaging*. 2013;6(10):1048–58.
- Luetkens JA, Doerner J, Thomas DK, et al. Acute myocarditis: multiparametric cardiac MR imaging. *Radiology*. 2014:132540.



15. Ferreira VM, Piechnik SK, Dall'Armellina E, et al. Native T1-mapping detects the location, extent and patterns of acute myocarditis without the need for gadolinium contrast agents. *J Cardiovasc Magn Reson*. 2014;16:36.
16. Mirakhor A, Anca N, Mikami Y, Merchant N. T2-weighted imaging of the heart – A pictorial review. *Eur J Radiol*. 2013;82(10):1755–62.
17. Burt JR, Zimmerman SL, Kamel IR, Halushka M, Bluemke DA. Myocardial T1 mapping: techniques and potential applications. *Radiographics*. 2014;34(2):377–95.
18. Miller C, Naish J, Shaw S, et al. 118 Multiparametric cardiovascular magnetic resonance surveillance of acute cardiac allograft rejection and characterisation of transplantation-associated myocardial injury. *Heart*. 2014;100(suppl 3):A67–8.
19. Mewton N, Liu CY, Croisille P, Bluemke D, Lima JA. Assessment of myocardial fibrosis with cardiovascular magnetic resonance. *J Am Coll Cardiol*. 2011;57(8):891–903.
20. Jellis CL, Kwon DH. Myocardial T1 mapping: modalities and clinical applications. *Cardiovasc Diagn Ther*. 2014;4(2):126–37.
21. Hwang SH, Choi BW. Advanced cardiac MR imaging for myocardial characterization and quantification: T1 mapping. *Korean Circ J*. 2013;43(1):1–6.
22. Dall'Armellina E, Ferreira VM, Kharbanda RK, et al. Diagnostic value of pre-contrast T1 mapping in acute and chronic myocardial infarction. *JACC Cardiovasc Imaging*. 2013;6(6):739–42.
23. von Knobelsdorff F, Prothmann M, Dieringer MA, et al. Differentiation of acute and chronic myocardial infarction using T2-weighted imaging, late enhancement and T1 and T2 mapping – a pilot study at 3T. *J Cardiovasc Magn Reson*. 2014;16(suppl 1):222.
24. Kali A, Cokic I, Tang RL, et al. Determination of location, size, and transmural extent of chronic myocardial infarction without exogenous contrast media by using cardiac magnetic resonance imaging at 3 T. *Circ Cardiovasc Imaging*. 2014;7(3):471–81.
25. Okur A, Kantarcı M, Kızrak Y, et al. Quantitative evaluation of ischemic myocardial scar tissue by noncontrast T1 mapping using 3 Tesla MR scanner. *Diagn Interv Radiol*. 2014;20:407–13. doi: 10.5152/dir.13520.
26. Bull S, White SK, Piechnik SK, et al. Human non-contrast T1 values and correlation with histology in diffuse fibrosis. *Heart*. 2013;99(13):932–7.
27. Lee SP, Lee W, Lee JM, et al. Assessment of diffuse myocardial fibrosis by using MR imaging in asymptomatic patients with aortic stenosis. *Radiology*. September 24, 2014;141120 (PubMed PMID: 25251584).
28. Su MY, Lin LY, Tseng YH, et al. CMR-verified diffuse myocardial fibrosis is associated with diastolic dysfunction in HFpEF. *JACC Cardiovasc Imaging*. 2014;7(10):991–7.
29. Puntmann VO, Voigt T, Chen Z, et al. Native T1 mapping in differentiation of normal myocardium from diffuse disease in hypertrophic and dilated cardiomyopathy. *JACC Cardiovasc Imaging*. 2013;6(4):475–84.
30. Dass S, Suttie JJ, Piechnik SK, et al. Myocardial tissue characterization using magnetic resonance non-contrast t1 mapping in hypertrophic and dilated cardiomyopathy. *Circ Cardiovasc Imaging*. 2012;5(6):726–33.
31. Broberg CS, Chugh SS, Conklin C, Sahn DJ, Jerosch-Herold M. Quantification of diffuse myocardial fibrosis and its association with myocardial dysfunction in congenital heart disease. *Circ Cardiovasc Imaging*. 2010;3(6):727–34.
32. Puntmann VO, D'Cruz D, Smith Z, et al. Native myocardial T1 mapping by cardiovascular magnetic resonance imaging in subclinical cardiomyopathy in patients with systemic lupus erythematosus. *Circ Cardiovasc Imaging*. 2013;6(2):295–301.
33. Ntusi NA, Piechnik SK, Francis JM, et al. Subclinical myocardial inflammation and diffuse fibrosis are common in systemic sclerosis—a clinical study using myocardial T1-mapping and extracellular volume quantification. *J Cardiovasc Magn Reson*. 2014;16:21.
34. Hosch W, Bock M, Libicher M, et al. MR-relaxometry of myocardial tissue: significant elevation of T1 and T2 relaxation times in cardiac amyloidosis. *Invest Radiol*. 2007;42(9):636–42.
35. Karamitsos TD, Piechnik SK, Banyersad SM, et al. Noncontrast T1 mapping for the diagnosis of cardiac amyloidosis. *JACC Cardiovasc Imaging*. 2013;6(4):488–97.
36. Fontana M, Banyersad SM, Treibel TA, et al. Native T1 mapping in transthyretin amyloidosis. *JACC Cardiovasc Imaging*. 2014;7(2):157–65.
37. Ruberg FL. T1 mapping in cardiac amyloidosis: can we get there from here? *JACC Cardiovasc Imaging*. 2013;6(4):498–500.
38. Sado DM, White SK, Piechnik SK, et al. Identification and assessment of Anderson-Fabry disease by cardiovascular magnetic resonance non-contrast myocardial T1 mapping. *Circ Cardiovasc Imaging*. 2013;6(3):392–8.
39. Sado DM, White SK, Piechnik SK, et al. Native T1 lowering in iron overload and Anderson Fabry disease; a novel and early marker of disease. *J Cardiovasc Magn Reson*. 2013;15(suppl 1):O71.
40. Sado DM, Maestrini V, Piechnik SK, et al. Noncontrast myocardial T1 mapping using cardiovascular magnetic resonance for iron overload. *J Magn Reson Imaging*. August 8, 2014. (doi: 10.1002/jmri.24727, PubMed PMID: 25104503).
41. Feng Y, He T, Carpenter JP, et al. In vivo comparison of myocardial T1 with T2 and T2* in thalassaemia major. *J Magn Reson Imaging*. 2013;38(3):588–93.
42. Kübler D, Gräfe M, Schnackenburg B, et al. T1 and T2 mapping for tissue characterization of cardiac myxoma. *Int J Cardiol*. 2013;169(1):e17–20.
43. Reiter U, Reiter G, Asslaber M, et al. Characterization of a calcified intra-cardiac pseudocyst of the mitral valve by magnetic resonance imaging including T1 and T2 mapping. *BMC Cardiovasc Disord*. 2014;14:11.
44. Ferreira VM, Holloway CJ, Piechnik SK, Karamitsos TD, Neubauer S. Is it really fat? Ask a T1-map. *Eur Heart J Cardiovasc Imaging*. 2013;14(11):1060.
45. Kramer CM, Chandrasekhar Y, Narula J. T1 mapping by CMR in cardiomyopathy: a noninvasive myocardial biopsy? *JACC Cardiovasc Imaging*. 2013;6(4):532–44.